NATIONAL ADVISORY COMMITTEE FOR AERONAUTICS

REPORT No. 647

TESTS OF N. A. C. A. 0009, 0012, AND 0018 AIRFOILS IN THE FULL-SCALE TUNNEL

By HARRY J. GOETT AND W. KENNETH BULLIVANT

1938

For sale by the Superintendent of Documents, Washington, D. C. - - - - - - - - - - - - - - Price 10 cents
Subscription price, $3 per year

AERONAUTIC SYMBOLS

1. FUNDAMENTAL AND DERIVED UNITS

	Symbol	Metric		English	
		Unit	Abbreviation	Unit	Abbreviation
Length	l	meter	m	foot (or mile)	ft. (or mi.)
Time	t	second	s	second (or hour)	sec. (or hr.)
Force	F	weight of 1 kilogram	kg	weight of 1 pound	lb.
Power	P	horsepower (metric)		horsepower	hp.
Speed	V	kilometers per hour	k.p.h.	miles per hour	m.p.h.
		meters per second	m.p.s.	feet per second	f.p.s.

2. GENERAL SYMBOLS

W, Weight$=mg$

g, Standard acceleration of gravity$=9.80665$ m/s^2 or 32.1740 ft./sec.^{2}

m, Mass$=\frac{W}{g}$

I, Moment of inertia$=mk^2$. (Indicate axis of radius of gyration k by proper subscript.)

μ, Coefficient of viscosity

ν, Kinematic viscosity

ρ, Density (mass per unit volume)

Standard density of dry air, 0.12497 kg-m^{-4}-s^2 at 15° C. and 760 mm; or 0.002378 lb.-ft.$^{-4}$ sec.^{2}

Specific weight of "standard" air, 1.2255 kg/m^3 or 0.07651 lb./cu. ft.

3. AERODYNAMIC SYMBOLS

S, Area

S_w, Area of wing

G, Gap

b, Span

c, Chord

$\frac{b^2}{S}$, Aspect ratio

V, True air speed

q, Dynamic pressure$=\frac{1}{2}\rho V^2$

L, Lift, absolute coefficient $C_L=\frac{L}{qS}$

D, Drag, absolute coefficient $C_D=\frac{D}{qS}$

D_0, Profile drag, absolute coefficient $C_{D_0}=\frac{D_0}{qS}$

D_i, Induced drag, absolute coefficient $C_{D_i}=\frac{D_i}{qS}$

D_p, Parasite drag, absolute coefficient $C_{D_p}=\frac{D_p}{qS}$

C, Cross-wind force, absolute coefficient $C_C=\frac{C}{qS}$

R, Resultant force

i_w, Angle of setting of wings (relative to thrust line)

i_t, Angle of stabilizer setting (relative to thrust line)

Q, Resultant moment

Ω, Resultant angular velocity

$\rho\frac{Vl}{\mu}$, Reynolds Number, where l is a linear dimension (e.g., for a model airfoil 3 in. chord, 100 m.p.h. normal pressure at 15° C., the corresponding number is 234,000; or for a model of 10 cm chord, 40 m.p.s., the corresponding number is 274,000)

C_p, Center-of-pressure coefficient (ratio of distance of c.p. from leading edge to chord length)

α, Angle of attack

ϵ, Angle of downwash

α_0, Angle of attack, infinite aspect ratio

α_i, Angle of attack, induced

α_a, Angle of attack, absolute (measured from zero-lift position)

γ, Flight-path angle

REPORT No. 647

TESTS OF N. A. C. A. 0009, 0012, AND 0018 AIRFOILS IN THE FULL-SCALE TUNNEL

By HARRY J. GOETT and W. KENNETH BULLIVANT

Langley Memorial Aeronautical Laboratory

108739—39

NATIONAL ADVISORY COMMITTEE FOR AERONAUTICS

HEADQUARTERS, NAVY BUILDING, WASHINGTON, D. C.

LABORATORIES, LANGLEY FIELD, VA.

Created by act of Congress approved March 3, 1915, for the supervision and direction of the scientific study of the problems of flight (U. S. Code, Title 50, Sec. 151). Its membership was increased to 15 by act approved March 2, 1929. The members are appointed by the President, and serve as such without compensation.

TECHNICAL COMMITTEES

AERODYNAMICS
POWER PLANTS FOR AIRCRAFT
AIRCRAFT MATERIALS
AIRCRAFT STRUCTURES
AIRCRAFT ACCIDENTS
INVENTIONS AND DESIGNS

Coordination of Research Needs of Military and Civil Aviation

Preparation of Research Programs

Allocation of Problems

Prevention of Duplication

Consideration of Inventions

LANGLEY MEMORIAL AERONAUTICAL LABORATORY

LANGLEY FIELD, VA.

Unified conduct, for all agencies, of scientific research on the fundamental problems of flight.

OFFICE OF AERONAUTICAL INTELLIGENCE

WASHINGTON, D. C.

Collection, classification, compilation, and dissemination of scientific and technical information on aeronautics.

REPORT No. 647

TESTS OF N. A. C. A. 0009, 0012, AND 0018 AIRFOILS IN THE FULL-SCALE TUNNEL

By Harry J. Goett and W. Kenneth Bullivant

SUMMARY

An investigation was conducted in the N. A. C. A. full-scale wind tunnel to determine the aerodynamic characteristics of the N. A. C. A. 0009, 0012, and 0018 airfoils, with the ultimate purpose of providing data to be used as a basis for comparison with other wind-tunnel data, mainly in the study of scale and turbulence effects. Three symmetrical 6- by 36-foot rectangular airfoils were used. The Reynolds Number range for minimum drag was from 1,800,000 to 7,000,000 and for maximum lift, from 1,700,000 to 4,500,000. The effect of rounded tips was determined for each of the airfoils. Tests were also made of the N. A. C. A. 0012 airfoil equipped with a 0.20c full-span split flap hinged at 0.80c. Tuft surveys were included to show the progressive breakdown of flow near maximum lift.

Momentum surveys were made in conjunction with force measurements at zero lift as an aid in converting force-test data to section coefficients.

INTRODUCTION

Since the inception of wind-tunnel testing, the problem of correcting and applying test results to full-scale flight conditions has existed. Theory indicates that no corrections are necessary when all the conditions of dynamic similitude are satisfied. One of the conditions of similarity, Reynolds Number, was met by the N. A. C. A. variable-density tunnel, in which tests are conducted at Reynolds Numbers in the lower flight range; however, experiments still revealed discrepancies due in part to dissimilarities in turbulence between wind tunnels and free air. Turbulence measurements in the N. A. C. A. wind tunnels resulted in the use of the "effective Reynolds Number" (references 1 and 2) in an attempt to improve the precision of applying data obtained in wind tunnels with high turbulence to flight conditions. The data upon which the effective Reynolds Number correction was based were, however, limited to conventional airfoils of medium thickness and did not include the variation of the effect of turbulence with thickness ratio and other airfoil characteristics. In order to provide data that would afford a broader basis for comparison and assist in improving the turbulence correction, the present investigation was conducted on symmetrical airfoils of N. A. C. A. 0009, 0012, and 0018 sections. The tests were made in the N. A. C. A. full-scale wind tunnel, which is known to have low turbulence and to provide a close approach to free-flight conditions.

In addition to force tests of the plain airfoils, the N. A. C. A. 0012 airfoil was tested with a 0.20c full-span split flap. The Reynolds Number range was from 1,700,000 to 7,000,000. Momentum measurements, made in the wakes of all three airfoils, were used to evaluate the drag caused by the airfoil tips and thus to obtain section drag characteristics. The data obtained in this investigation are presented in order to make them available for comparison and analysis.

EQUIPMENT AND AIRFOILS

A description of the full-scale wind tunnel and of its test equipment is given in reference 3. The turbulence factor of the tunnel as determined by sphere tests is 1.1 (reference 1).

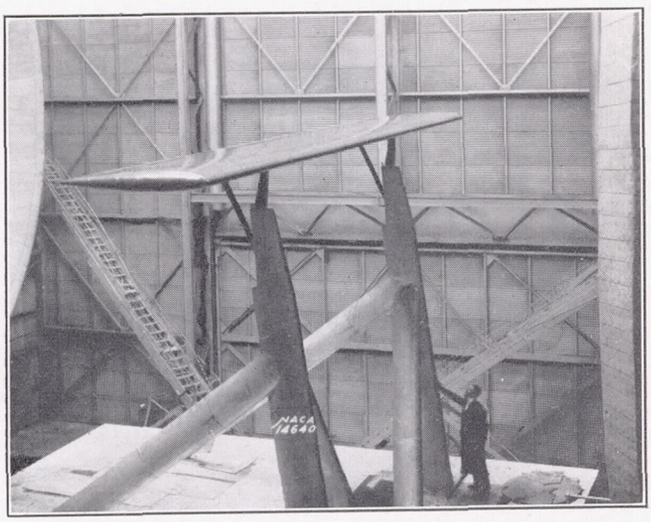

FIGURE 1.—The N. A. C. A. 0012 airfoil mounted in the full-scale wind tunnel.

During the tests, the airfoils were mounted with the main support attached at the quarter-chord point of the airfoils (fig. 1). The angle of attack was changed by a vertical movement of the lower ends of the rear supports.

Three 6- by 36-foot rectangular airfoils having N. A. C. A. 0009, 0012, and 0018 symmetrical sections were constructed for these tests. The airfoils were of

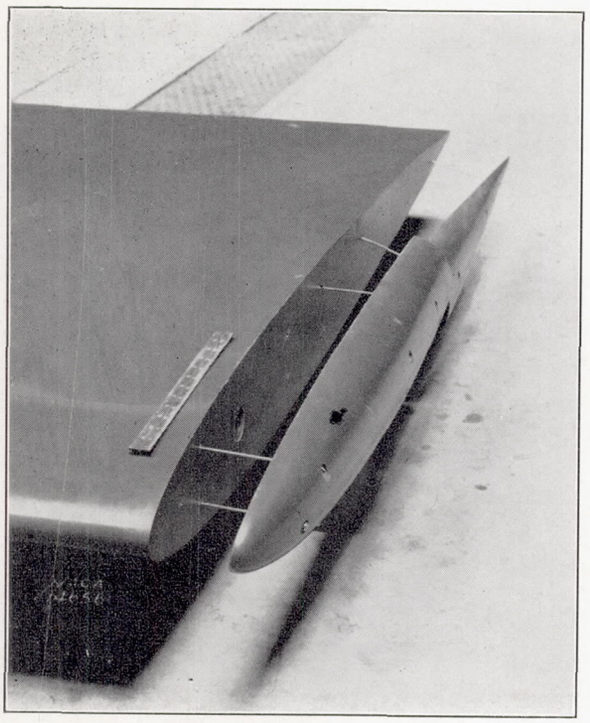

FIGURE 2.—Detachable rounded tip for the N. A. C. A. 0009 airfoil.

steel-spar construction with ribs spaced at 12-inch intervals. The covering was $\frac{1}{16}$-inch aluminum sheets, attached with countersunk screws. The seams and

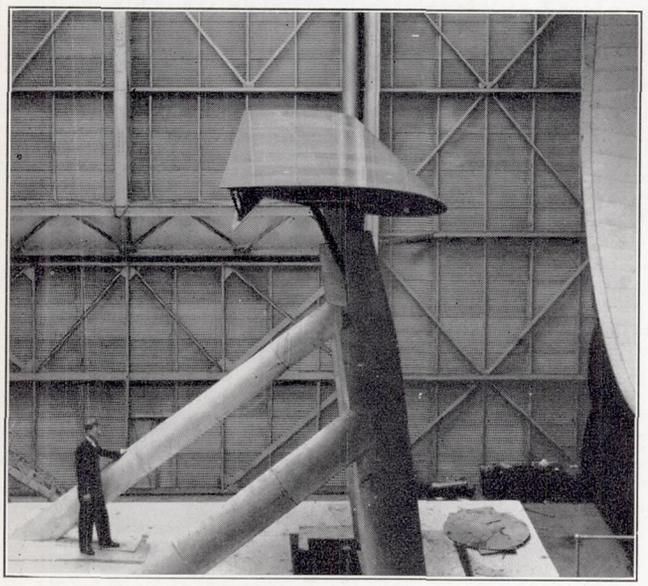

FIGURE 3.—The N. A. C. A. 0012 airfoil with 0.20c full-span split flap.

the screw slots were filled and the entire surface was then sanded, coated with paint primer, and polished to a glossy, wax-like finish. Tolerances on the section ordinates were kept within $\pm\frac{1}{32}$ inch.

Detachable rounded tips were provided for each airfoil. These tips, shown in figure 2, formed one-half of a solid of revolution, the radius at each chordwise station being equal to one-half of the local airfoil thickness.

A full-span 0.20c split flap constructed of $\frac{1}{4}$-inch plywood was provided for the N. A. C. A. 0012 airfoil. Figure 3 shows the flap mounted on the airfoil.

The rack used for the momentum measurements (fig. 4) consisted of a comb of total-head tubes and a comb of static tubes. These combs were placed 6 inches apart and the entire assembly was mounted on the survey carriage. The detailed spacing and the

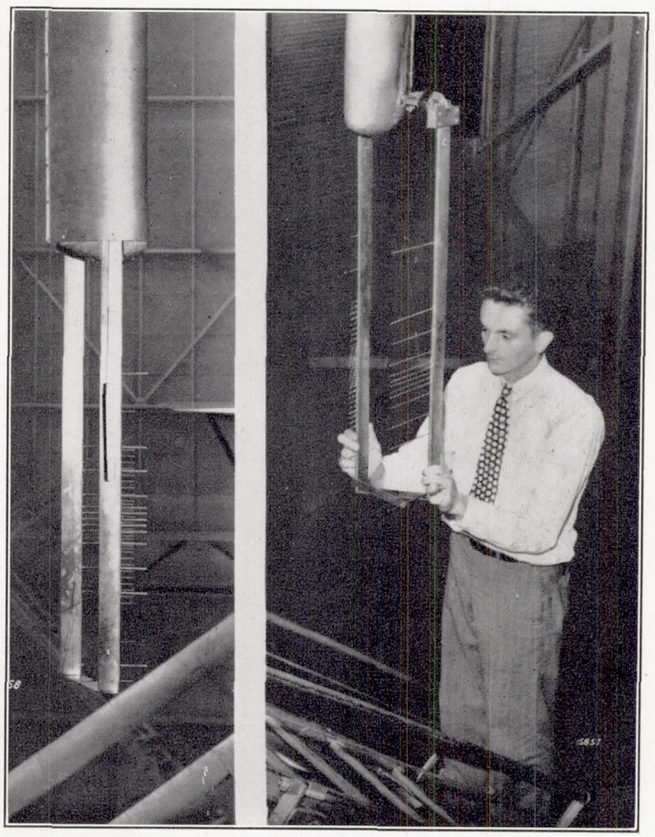

FIGURE 4.—Views of the rack used for momentum measurements.

dimensions of both combs are shown in figure 5. The total-head comb consisted of 39 tubes of 0.065-inch outside diameter by 0.036-inch inside diameter; the static comb consisted of 13 tubes of 0.125-inch outside diameter. Each tube was connected to the multiple-tube, photographic-recording manometer carried in the survey carriage.

TESTS

Tare and interference were evaluated by preliminary tests of the airfoils. The tare tests to determine the air forces on the supports were made with the airfoil supported independently of the balance by cables. The interference of the supports on the air flow was measured by adding two dummy support struts, shown in figure 6, which were free from contact with the airfoils.

Lift, drag, and pitching moments of the airfoils with square tips were measured at test velocities from 25 to 118 miles per hour over a range of angles of attack from −7° to 27°. Similar runs were made with the rounded tips on the airfoils at a sufficient number of speeds to afford comparison with the tests of the airfoils with square tips. The N. A. C. A. 0012 airfoil was also tested with a 0.20c full-span split flap deflected 15°, 30°, 45°, and 60°. Wool tufts were used to indicate the progression of the stall on the upper surfaces of the airfoils.

By means of the rack previously described, simultaneous measurements were made of the total and the static pressures in the wakes of the airfoils for the zero-lift condition. The measurements were made 15 percent of the chord behind the trailing edge at 27 spanwise locations.

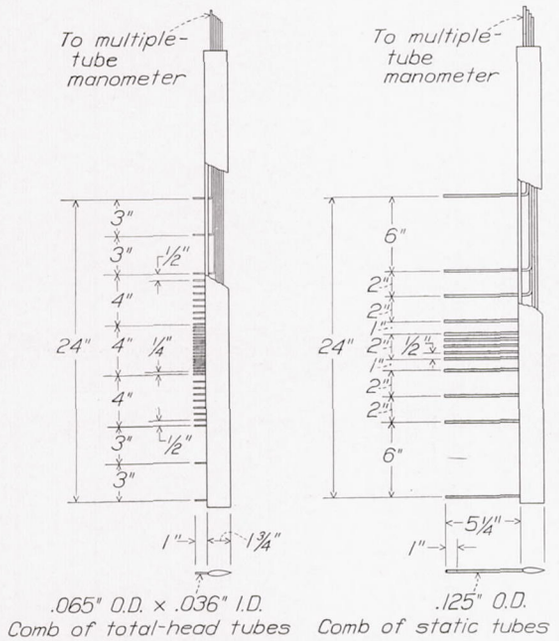

FIGURE 5.—Combs of total-head tubes and static tubes.

REDUCTION OF DATA

The measured wind-tunnel data were corrected in the following manner:

Dynamic pressure was determined from the difference in static pressure between two points in the tunnel. This difference was correlated with the free-stream dynamic pressure at the airfoil location (jet empty); the correlation was then modified for the blocking effect of the airfoil, as outlined in reference 4.

In the computation of the coefficients for the airfoils with rounded tips, the added area of the tips was not included. All coefficients are thus based on the original rectangular area of the square-tip airfoils.

Tare and interference coefficients were deducted from the gross coefficients. Owing to the small portions of the supporting struts exposed to the air stream, the tare drag is only about 7 percent of the net minimum drag of the airfoils at a test speed of 100 miles per hour. The interference correction was larger; for the thickest airfoil, interference drag was equal to 13 percent of the net drag for the test speed of 100 miles per hour. A small tare and interference correction was required for the pitching moment, but no correction was required for lift.

Pitch-angle surveys in the region of the jet occupied by the airfoils showed an average stream downflow of 0.6°. This value was corroborated by the force tests in that the angle of zero lift was 0.6° with respect to the tunnel axis. Because the scales measured force components perpendicular and parallel to the tunnel axis, these components were corrected to obtain true lift and drag components with reference to the air stream.

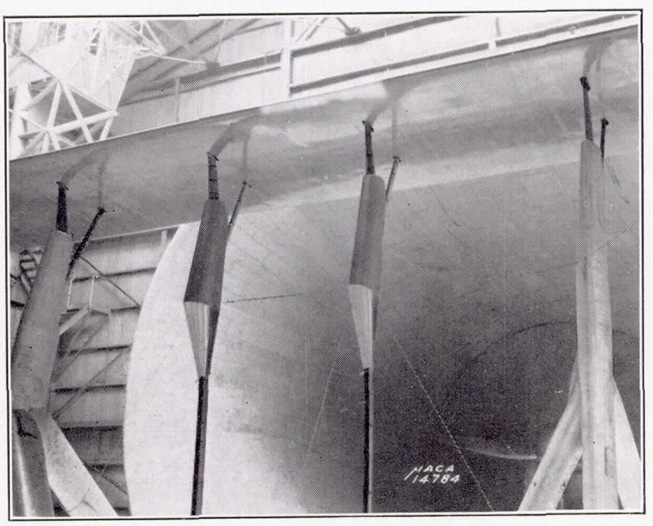

FIGURE 6.—Dummy supports added to the N. A. C. A. 0009 airfoil set-up for the interference tests.

The jet-boundary corrections, as evaluated for the full-scale tunnel in reference 4, were applied.

Coefficients for infinite aspect ratio were derived from the corrected results of the tests of the rounded-tip airfoils of aspect ratio 6 by the formulas:

$$\alpha_0=\alpha-\frac{C_L}{\pi A}(1+\tau)57.3$$

$$C_{D_0}=C_D-\frac{C_L^2}{\pi A}(1+\sigma)$$

where

$_0$ is angle of attack for infinite aspect ratio, degrees.
C_D, profile-drag coefficient.
A, aspect ratio.
τ, a factor correcting the induced angle of attack to allow for the change from elliptical span loading to a span loading for an airfoil with rectangular plan form.

σ, a factor correcting the induced drag to allow for the change from elliptical span loading to a span loading for an airfoil with rectangular plan form.

Values of $\tau=0.176$ and $\sigma=0.051$ for aspect ratio 6 were obtained from figure 7 of reference 5.

A deduction for the tip drag obtained from the momentum measurements was also made to obtain the true section drag. (The variation in this correction with thickness ratio for both rounded-tip and square-tip airfoils is shown in fig. 17.) This correction is strictly valid only at the angle of zero lift but is assumed constant throughout the entire angle-of-attack range.

No correction is required for static-pressure gradient in the stream jet because it is so small that the resulting decrement in drag is within the precision of the scales.

No effective Reynolds Number correction is applied because (1) maximum lift coefficients obtained on airplanes in flight and in the full-scale tunnel are in good agreement (references 2, 3, and 6); and (2) there are no known corrections to be applied to profile drag for the small amount of turbulence existing in the jet of the full-scale wind tunnel. An investigation is now being made in which it is planned to compare the section profile-drag coefficients obtained by the momentum method in flight and in the tunnel.

The computation of the section profile-drag coefficients from the momentum data was based on the theory given in the appendix. The formula used was

$$c_{d_0}=2\int\frac{\sqrt{H-P}}{\sqrt{H_0-P_0}}\left(1-\frac{\sqrt{H-P_0}}{\sqrt{H_0-P_0}}\right)d(y/c)$$

where

H is the total pressure in the wake.

P, static pressure in the wake.

H_0, free-stream total pressure.

P_0, free-stream static pressure.

y, vertical displacement from the trailing edge of the airfoil.

c, airfoil chord.

The method of computation was as follows:

1. The values of H and P were determined from faired curves of total and static pressures across the wake profile, to which a correction was applied to allow for the vertical gradients existing in the tunnel. The values of H_0 and P_0 were determined from total-head- and static-tube readings taken well outside the wake with a proper calibration applied to obtain the free-stream values of these quantities.

2. The quantity

$$2\frac{\sqrt{H-P}}{\sqrt{H_0-P_0}}\left(1-\frac{\sqrt{H-P_0}}{\sqrt{H_0-P_0}}\right)$$

was then plotted against y/c. This curve was integrated, the summation being the section profile-drag coefficient at the station of measurement.

ACCURACY

An estimate follows of the precision of the final results, based upon a consideration of the accuracy of the measurements of air-stream velocity, balance readings, and angle-of-attack setting and the probable errors in the applied corrections.

α, $\pm 0.1°$.

$C_{L_{max}}$, ± 0.03.

$\frac{dC_L}{d\alpha}$, ± 0.0015 per degree.

C_{D_0}, ± 0.0002 ($C_L=0$).

C_{D_0}, ± 0.0015 ($C_L=1.0$).

$C_{m_{c/4}}$, ± 0.003.

RESULTS AND DISCUSSION

The principal aerodynamic characteristics of the N. A. C. A. 0009, 0012, and 0018 square-tip airfoils of aspect ratio 6 are given in figures 7, 8, and 9 for an average Reynolds Number of 3,400,000. Lift and drag coefficients for the airfoils with rounded tips are also given. The corresponding section characteristics are presented in figure 10. Table I gives a summary of the results for the square-tip airfoils over a Reynolds Number range from 1,700,000 to 7,000,000.

TABLE I

IMPORTANT CHARACTERISTICS OF SQUARE-TIP AIRFOILS OF ASPECT RATIO 6

N. A. C. A. airfoil	Reynolds Number (millions)	$C_{L_{max}}$	α at $C_{L_{max}}$ (deg.)	$\frac{dC_L}{d\alpha}$	$C_{D_{min}}$	$\left(\frac{L}{D}\right)_{max}$
0009	1.8	1.09	16.2	0.071	0.0066	------
	3.0	1.20	17.1	.071	.0062	24.9
	5.0	1.26	17.7	.071	.0060	------
	7.0	----------	----------	.072	.0058	------
0012	1.8	1.22	17.6	.072	.0071	------
	3.0	1.33	18.9	.072	.0069	24.7
	5.0	----------	----------	.073	.0066	------
	7.0	----------	----------	.074	.0064	------
0018	1.8	1.15	17.8	.070	.0091	------
	3.0	1.26	18.4	.071	.0085	21.0
	5.0	1.36	19.6	.072	.0082	------
	7.0	----------	----------	.073	.0078	------
0012; 60°, 0.20c split flap	1.7	2.10	17.7	----------	----------	5.1
	2.2	2.14	18.2	----------	----------	5.2
	3.0	2.21	19.6	.074	----------	5.2
	4.0	2.28	20.4	----------	----------	5.2

Figures 7 to 9 show a marked decrease in the sharpness of the stall of the N. A. C. A. 0018 airfoil as compared with the thinner sections. Figures 11, 12, and 13, which show the history of the flow in the region of the stall for the three airfoils, offer an explanation of this phenomenon. It will be noted that, for the N. A. C. A. 0018 airfoil, the initial breakaway of flow precedes the angle of attack at maximum lift to a greater extent than it does for the N. A. C. A. 0009 and 0012 airfoils and that the spread of the stalled region is much more gradual. The lack of a "hysteresis" loop for the N. A. C. A. 0018 airfoil may also be explained by the fact that the unstalled flow is more readily reestablished on an airfoil which stalls "gradually." Comparisons of force tests with and without tufts show negligible differences, justifying the assumption that the tufts cause no important change in the character of the flow.

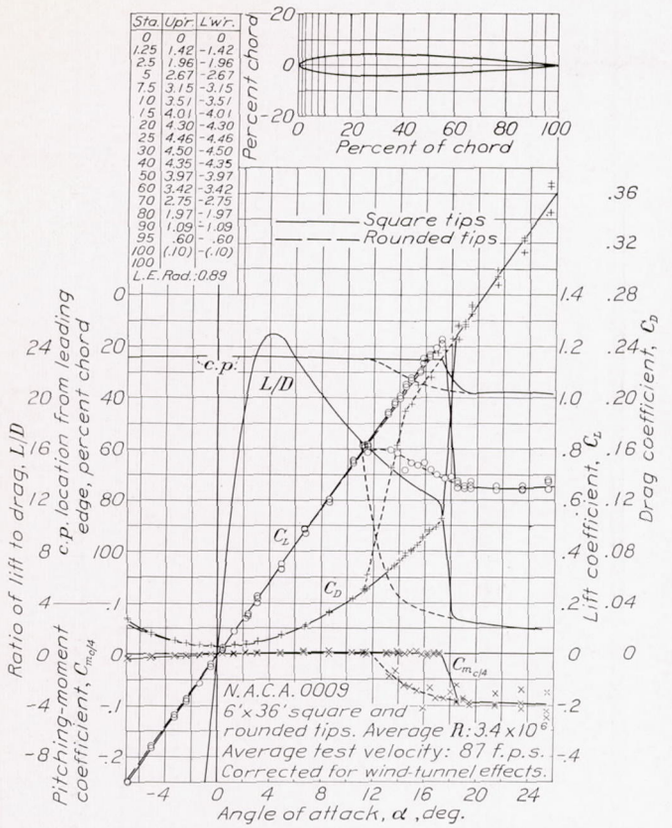

FIGURE 7.—Characteristics of the N. A. C. A. 0009 airfoil of aspect ratio 6.

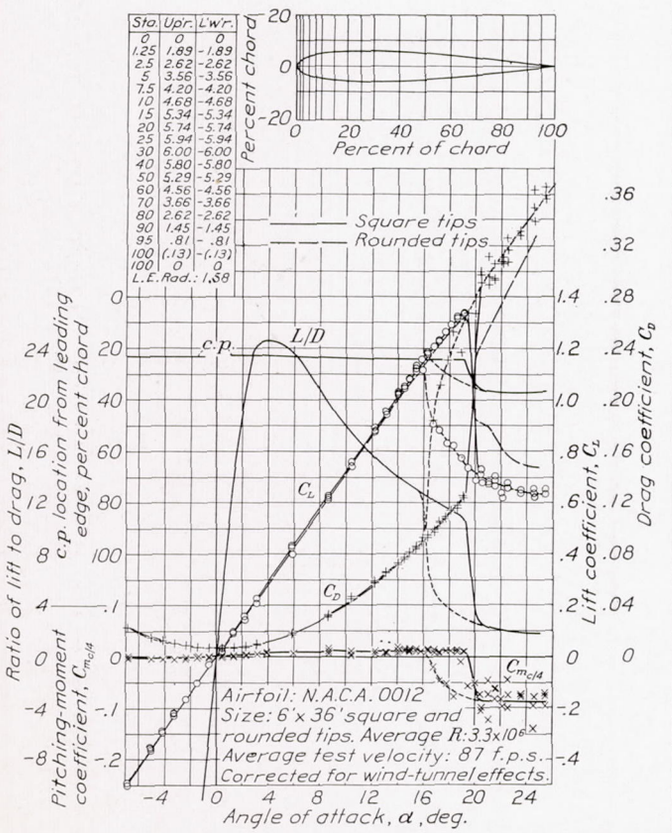

FIGURE 8.—Characteristics of the N. A. C. A. 0012 airfoil of aspect ratio 6.

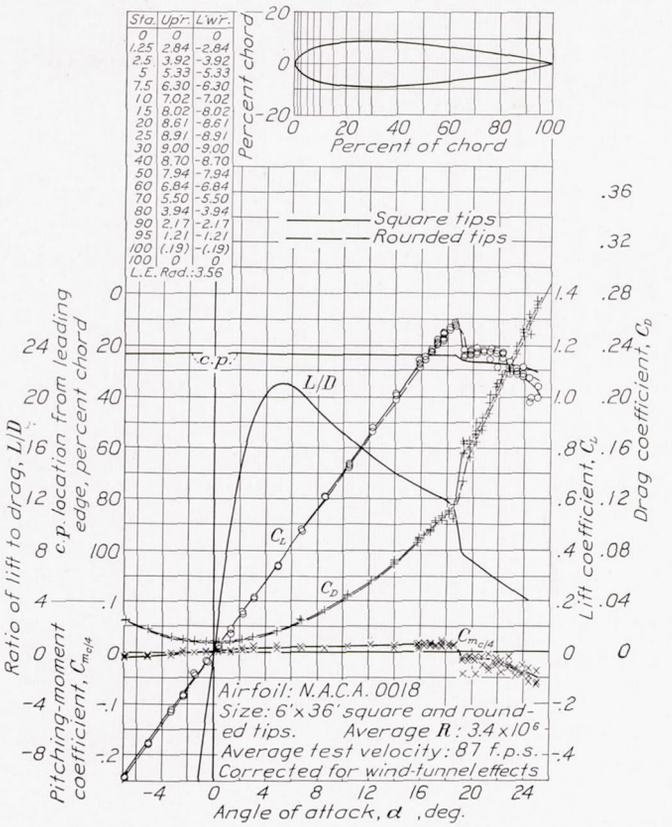

FIGURE 9.—Characteristics of the N. A. C. A. 0018 airfoil of aspect ratio 6.

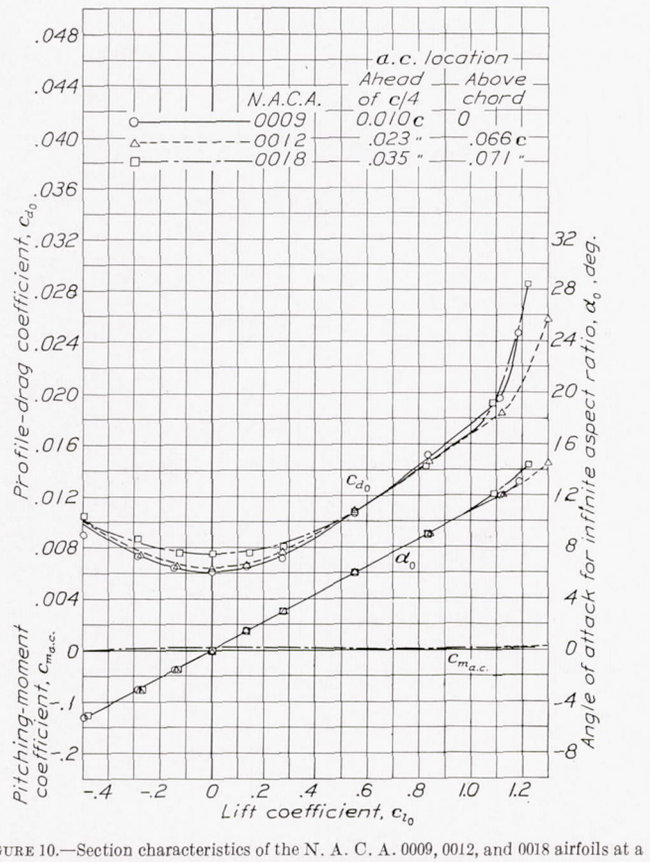

FIGURE 10.—Section characteristics of the N. A. C. A. 0009, 0012, and 0018 airfoils at a Reynolds Number of 3,400,000.

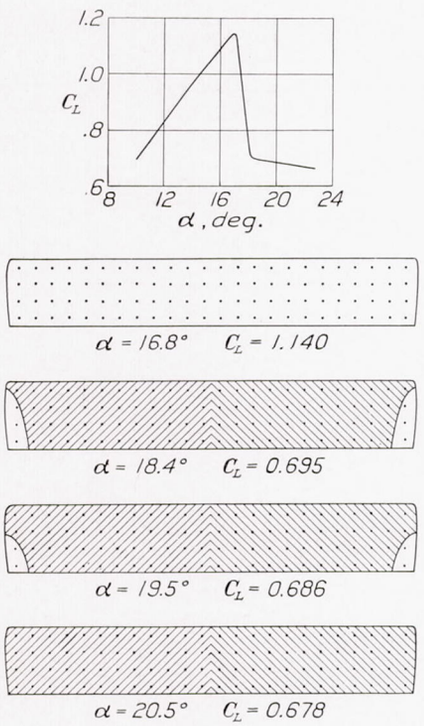

FIGURE 11.—The N. A. C. A. 0009 airfoil.

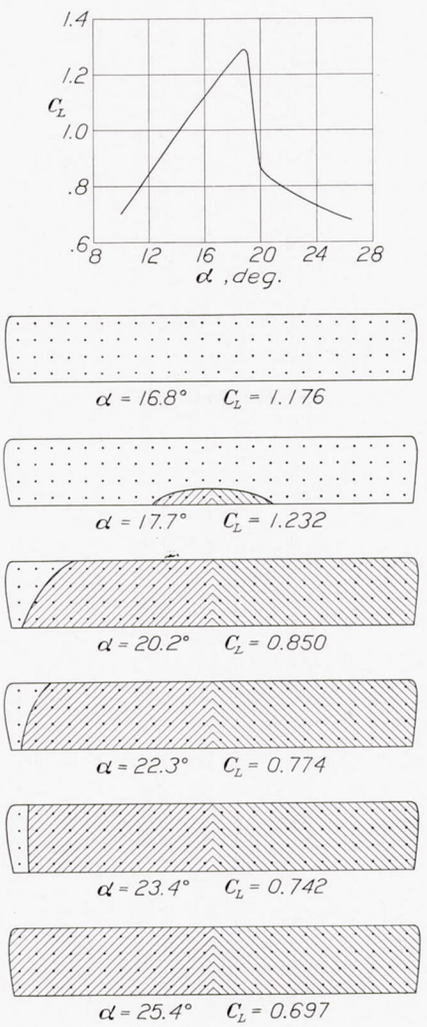

FIGURE 12.—The N. A. C. A. 0012 airfoil.

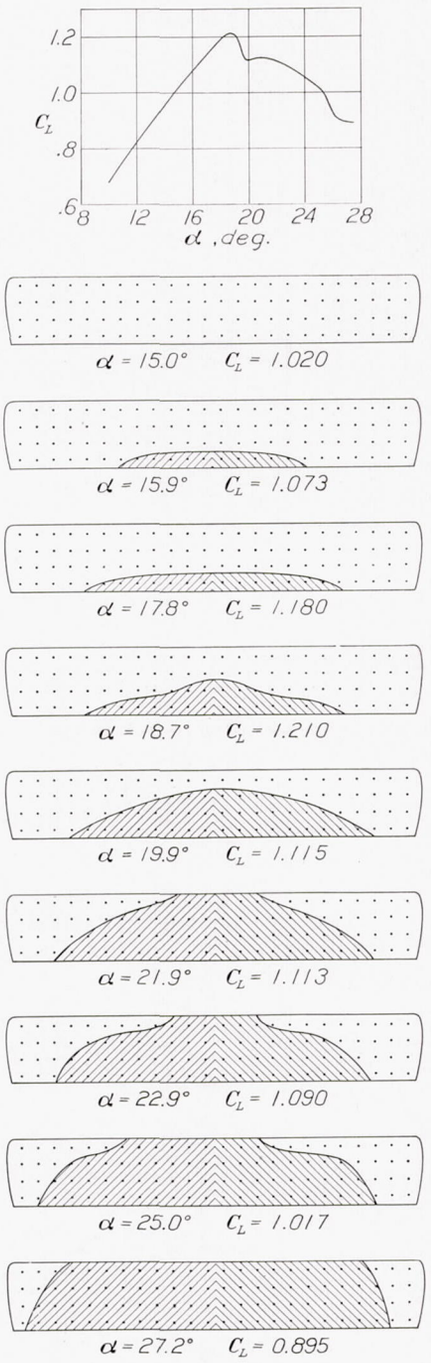

FIGURE 13.—The N. A. C. A. 0018 airfoil.

FIGURES 11 TO 13.—Stalling contours of three N. A. C. A. airfoils with rounded tips. Approximate test velocity, 84 f. p. s. Cross-hatched areas indicate stalled region.

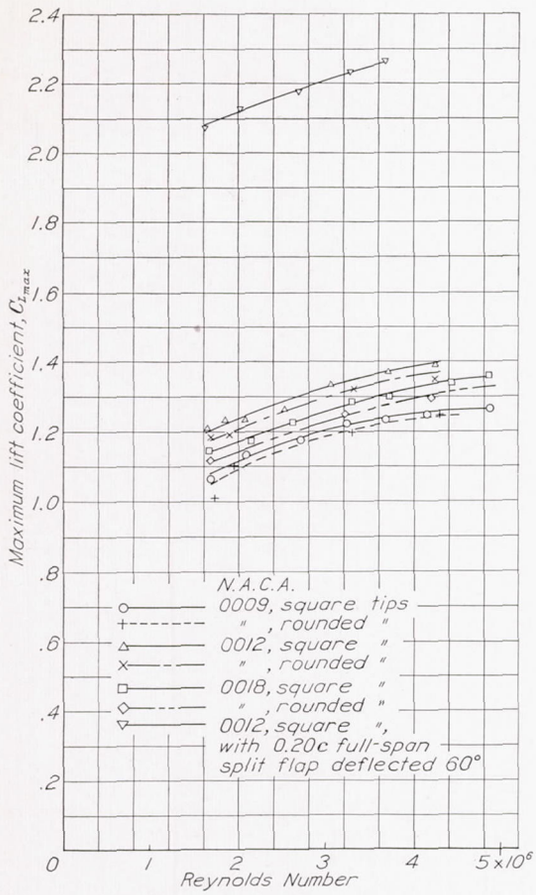

FIGURE 14.—Variation of maximum lift with Reynolds Number for the N. A. C. A. 0009, 0012, and 0018 airfoils of aspect ratio 6.

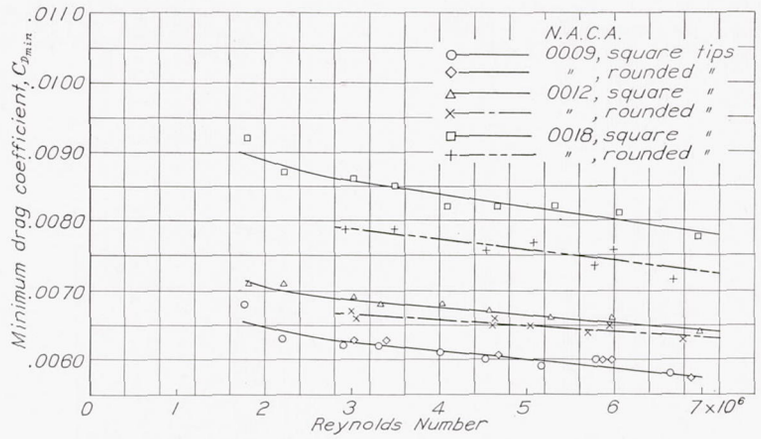

FIGURE 15.—Variation of minimum drag with Reynolds Number for the N. A. C. A. 0009, 0012, and 0018 airfoils of aspect ratio 6.

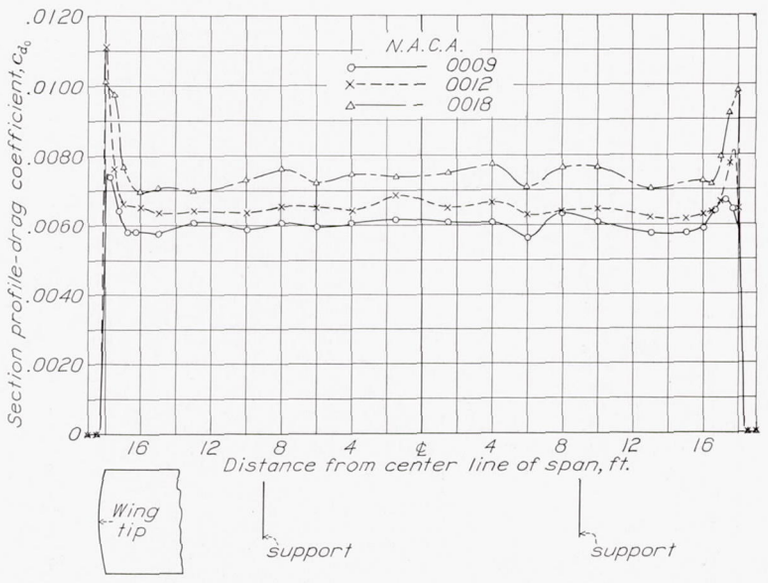

FIGURE 16.—Variation of section profile-drag coefficient across the spans of three rounded-tip airfoils of aspect ratio 6 at zero lift.

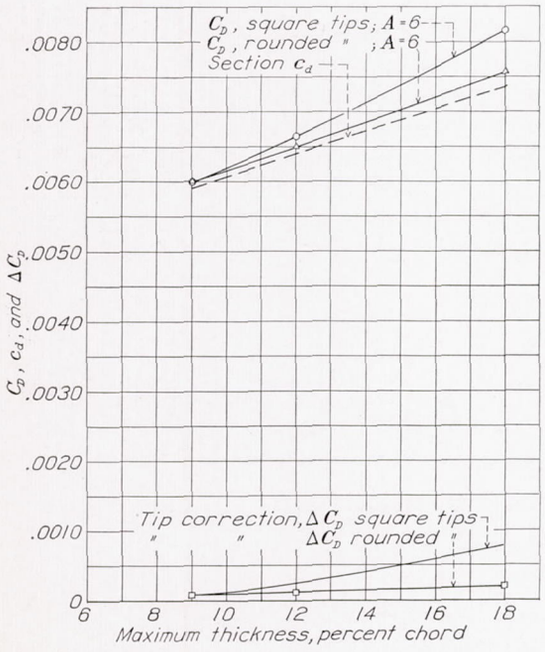

FIGURE 17.—Effect of thickness on profile-drag coefficient and tip correction for airfoils of aspect ratio 6 at zero lift and at a Reynolds Number of 5,000,000.

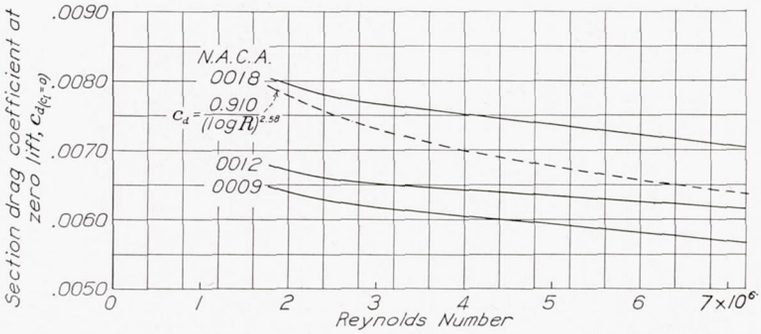

FIGURE 18.—Variation of section drag coefficient with Reynolds Number for three airfoils of aspect ratio 6 at zero lift.

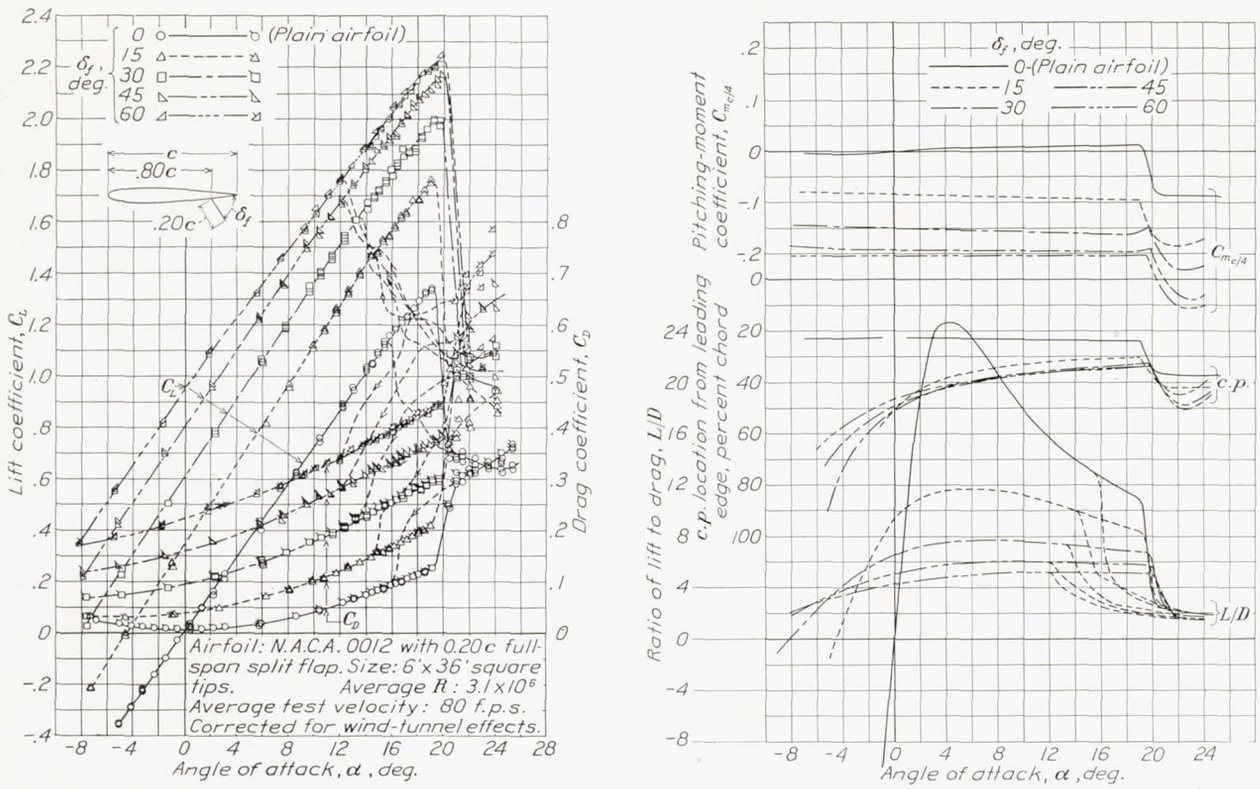

FIGURE 19.—Characteristics of the square-tip N. A. C. A. 0012 airfoil of aspect ratio 6 with a 0.20c full-span split flap.

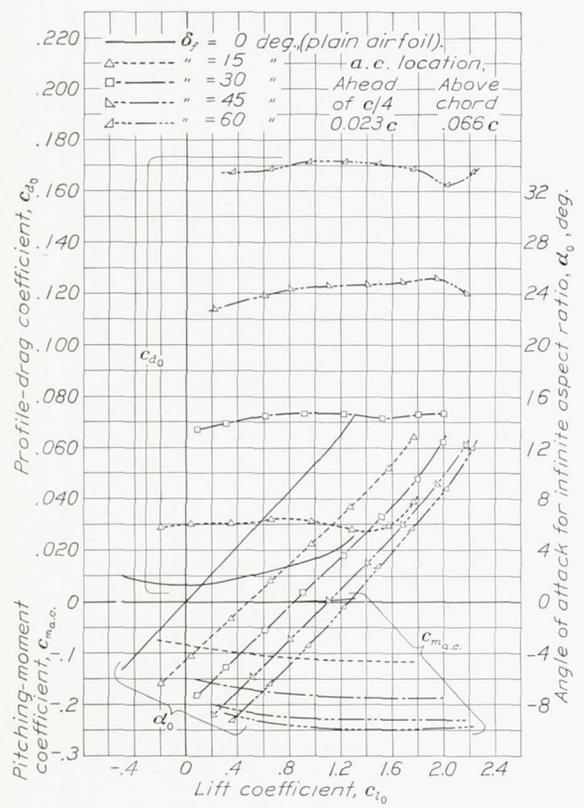

FIGURE 20.—Section characteristics of the N. A. C. A. 0012 airfoil with a 0.20c full-span split flap at a Reynolds Number of 3,100,000.

The effect of Reynolds Number on the maximum lift and the minimum drag coefficients of the three airfoils and of the N. A. C. A. 0012 airfoil with the 0.20c full-span split flap deflected 60° is shown in figures 14 and 15. It will be noted that the addition of the rounded tips to the airfoils causes a decrease in the maximum lift coefficient varying from about 2.5 percent for the N. A. C. A. 0018 airfoil to about 1.5 percent for the N. A. C. A. 0009 airfoil.

The variation in section profile-drag coefficient across the span of the three rounded-tip airfoils, as measured at zero lift by the momentum method, is shown in figure 16. The over-all profile drag obtained by an integration across the span of the airfoils compares with that measured by force tests, as shown in table II.

TABLE II

COMPARISON OF PROFILE-DRAG COEFFICIENTS FOR THE ROUNDED-TIP AIRFOILS OF ASPECT RATIO 6 OBTAINED AT ZERO LIFT BY THE FORCE TESTS AND THE MOMENTUM METHOD. R=5,000,000

N. A. C. A. airfoil	C_{D_0}	
	Momentum test	Force test
0009	0.0061	0.0060
0012	.0066	.0065
0018	.0075	.0076

This agreement is within the experimental accuracy of the momentum method and is sufficient to warrant the conclusion that this method satisfactorily measures profile drag at zero lift. The maximum variation of ± 0.0002, which will be noted in the individual section coefficients across the span of the airfoils (fig. 16), is attributed to a combination of experimental error and unavoidable differences that existed in the surfaces at the various stations. Designers should note that the airfoils used for this investigation, as in all wind-tunnel investigations of airfoil characteristics, were appreciably smoother than wings commonly used in airplane construction.

The increase in drag caused by the rounded tips, shown in figure 16, indicates that something in excess of the section drag is measured by the force test. A comparison between the over-all profile-drag coefficient of the airfoil of aspect ratio 6 and the section profile-drag coefficient is shown in table III. The section profile drag was considered the average across the airfoil inboard of the area affected by the tips. The correction for the tip drag is thus derived from the difference between the section and the over-all profile-drag coefficients. The section drag is obtained by deducting the tip correction shown in figure 17 and given in table III from the force-test results obtained for the rounded-tip airfoil. No appreciable variation in tip drag was noted over a range of Reynolds Numbers between 3,000,000 and 5,000,000.

TABLE III

TIP CORRECTIONS FOR THE ROUNDED-TIP AIRFOILS OF ASPECT RATIO 6 FROM MOMENTUM TEST. R=5,000,000

N. A. C. A. airfoil	C_{D_0}	c_{d_0}	Rounded-tip drag, ΔC_D
0009	0.0061	0.0060	0.0001
0012	.0066	.0065	.0001
0018	.0075	.0073	.0002

Figure 17 also shows the variation of this tip correction with profile thickness for the square-tip airfoils of aspect ratio 6. The supplementary drag caused by the square tips varies from zero for the airfoil of 9 percent thickness to 13 percent of the minimum drag for the airfoil of 18 percent thickness. Thus the results for square-tip airfoils, when uncorrected for tip drag, greatly magnify the increase of drag with profile thickness.

Figure 18 gives the variation of section drag at zero lift with Reynolds Number, obtained by applying the proper tip correction to the results given in figure 15.

The aerodynamic characteristics of the N. A. C. A. 0012 airfoil with the full-span $0.20c$ split flap for flap deflections of 0°, 15°, 30°, 45°, and 60° at a Reynolds Number of 3,100,000 are given in figure 19. Figure

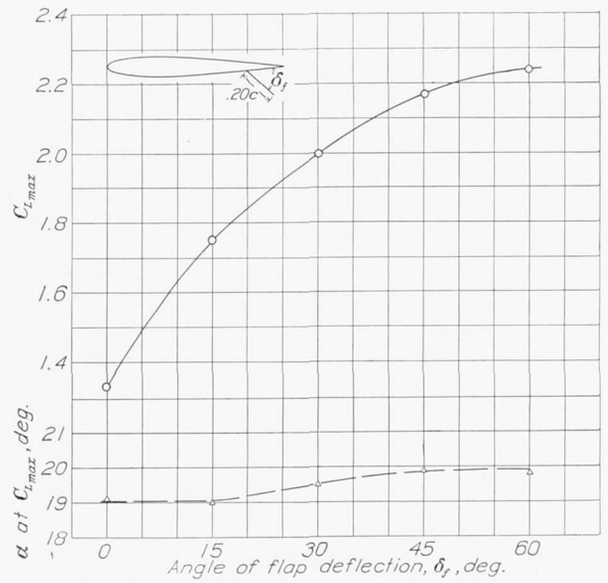

FIGURE 21.—Variation of maximum lift and angle of attack at maximum lift with flap deflection at a Reynolds Number of 3,100,000 for the square-tip N. A. C. A. 0012 airfoil of aspect ratio 6.

20 gives the corresponding section characteristics and figure 21 shows the variation of the maximum lift coefficient and of the angle of attack at maximum lift with flap deflection.

At the present time, the data herein presented and those available from other sources are being compared with a view toward determining the cause and magnitude of existing discrepancies.

LANGLEY MEMORIAL AERONAUTICAL LABORATORY,
NATIONAL ADVISORY COMMITTEE FOR AERONAUTICS,
LANGLEY FIELD, VA., *July 28, 1938.*

APPENDIX

The computation of drag from the momentum data was made by the method developed by B. Melville Jones (reference 7). A comparison was made between the drag values given by this method and those given by the method developed by Betz (reference 8). The maximum difference in the profile-drag coefficient was found to be no greater than ± 0.0001, when the computations were based on the same data. The Jones method was used because of the greater simplicity of the computations required.

Except for minor changes in notation, the derivation of the Jones momentum equation, as developed in reference 7, is as follows:

Consider an airfoil in a free stream of velocity U, with a drag D and no force component perpendicular to U. The drag experienced by the body will be caused by the change in momentum that the body imposes on the free stream. Thus in a plane AA (fig. 22), far behind the body where the static pressure

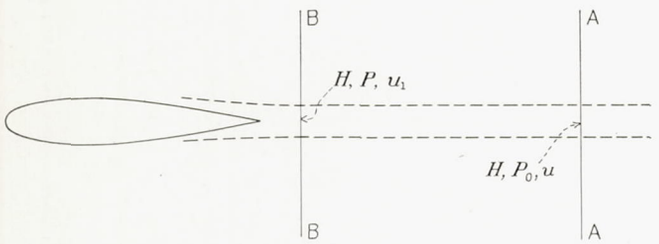

FIGURE 22.—Diagram of airfoil and wake.

is equal to that of the free stream and the velocity is parallel to U, the magnitude of the velocity is everywhere equal to U except in a well-defined wake region where it is less than U. If da is an element of area in the plane AA in the wake where the air velocity is u, the drag D is given by the equation

$$D=\rho \int\int u(U-u)da \tag{1}$$

The actual measurements are to be made in the plane BB, where the static pressure is in excess of that of the free stream. Then the mass flow across an element da_1, in the plane BB, where the velocity is u_1, is $\rho u_1 da_1$ (neglecting the effect of angularity, which will be small). If the symbol u is retained for the velocity of flow in this tube where it passes through plane AA, the drag, which is equal to the defect of momentum crossing the whole plane AA in unit time, is given by

$$D=\rho \int\int u_1(U-u)da_1 \tag{2}$$

The assumption that *no loss of total pressure occurs in the tubes of flow between* BB *and* AA permits the final velocity u to be determined from the total pressure at section BB and the free-stream static pressure. In the actual flow, there is a mixing that causes a widening out of the wake as the distance from the trailing edge increases. The method presumes that this difference between the real and the imagined flow does not influence the drag.

In order to use equation (2), it must be expressed in terms of the total- and the static-pressure measurements that will actually be made. These measurements will be:

H, total pressure in wake at plane BB.
P, static pressure in wake at plane BB.
H_0, free-stream total pressure.
P_0, free-stream static pressure.
y, vertical displacement from trailing edge of airfoil.

Then

$$H_0-P_0=\frac{1}{2}\rho U^2$$

$$H-P=\frac{1}{2}\rho u_1^2$$

$$H-P_0=\frac{1}{2}\rho u^2$$

Substituting for U, u_1, and u

$$D=2\int\int \sqrt{H-P}\left(\sqrt{H_0-P_0}-\sqrt{H-P_0}\right)da_1 \tag{3}$$

Reduced to coefficient form, equation (3) becomes

$$c_{d_0}=2\int \frac{\sqrt{H-P}}{\sqrt{H_0-P_0}}\left(1-\frac{\sqrt{H-P_0}}{\sqrt{H_0-P_0}}\right)d(y/c) \tag{4}$$

This equation was used in the computation of drag from the momentum data.

REFERENCES

1. Platt, Robert C.: Turbulence Factors of N. A. C. A. Wind Tunnels as Determined by Sphere Tests. T. R. No. 558, N. A. C. A., 1936.
2. Jacobs, Eastman N., and Clay, William C.: Characteristics of the N. A. C. A. 23012 Airfoil from Tests in the Full-Scale and Variable-Density Tunnels. T. R. No. 530, N. A. C. A., 1935.
3. DeFrance, Smith J.: The N. A. C. A. Full-Scale Wind Tunnel. T. R. No. 459, N. A. C. A., 1933.
4. Theodorsen, Theodore, and Silverstein, Abe: Experimental Verification of the Theory of Wind-Tunnel Boundary Interference. T. R. No. 478, N. A. C. A., 1934.
5. Silverstein, Abe: Scale Effect on Clark Y Airfoil Characteristics from N. A. C. A. Full-Scale Wind-Tunnel Tests. T. R. No. 502, N. A. C. A., 1934.
6. Silverstein, Abe, Katzoff, S., and Hootman, James H.: Comparative Flight and Full-Scale Wind-Tunnel Measurements of the Maximum Lift of an Airplane. T. R. No. 618, N. A. C. A., 1938.
7. The Cambridge University Aeronautics Laboratory (B. Melville Jones): Measurement of Profile Drag by the Pitot-Traverse Method. R. & M. No. 1688, British A. R. C., 1936.
8. Betz, A.: A Method for the Direct Determination of Wing-Section Drag. T. M. No. 337, N. A. C. A., 1925.

U. S. GOVERNMENT PRINTING OFFICE: 1939

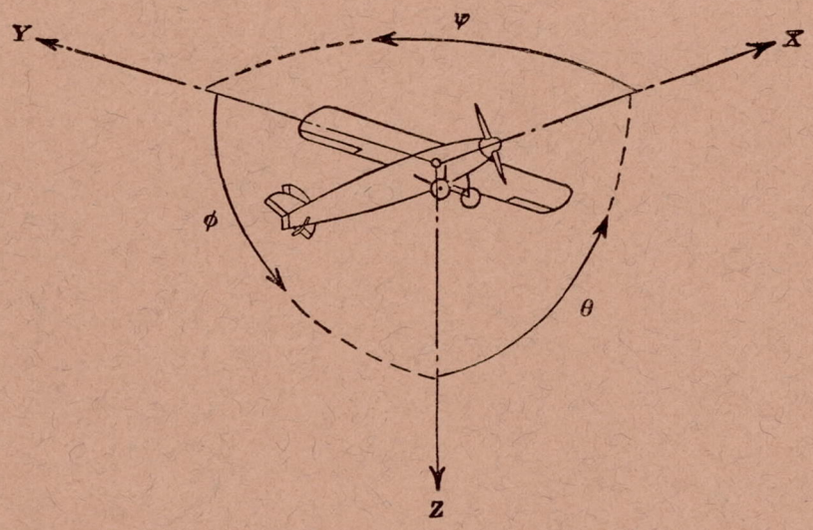

Positive directions of axes and angles (forces and moments) are shown by arrows

Axis		Force (parallel to axis) symbol	Moment about axis			Angle		Velocities	
Designation	Symbol		Designation	Symbol	Positive direction	Designation	Symbol	Linear (component along axis)	Angular
Longitudinal	X	X	Rolling	L	$Y \longrightarrow Z$	Roll	ϕ	u	p
Lateral	Y	Y	Pitching	M	$Z \longrightarrow X$	Pitch	θ	v	q
Normal	Z	Z	Yawing	N	$X \longrightarrow Y$	Yaw	ψ	w	r

Absolute coefficients of moment

$C_l = \frac{L}{qbS}$ (rolling) $\quad C_m = \frac{M}{qcS}$ (pitching) $\quad C_n = \frac{N}{qbS}$ (yawing)

Angle of set of control surface (relative to neutral position), δ. (Indicate surface by proper subscript.)

4. PROPELLER SYMBOLS

D, Diameter

p, Geometric pitch

p/D, Pitch ratio

V', Inflow velocity

V_s, Slipstream velocity

T, Thrust, absolute coefficient $C_T = \frac{T}{\rho n^2 D^4}$

Q, Torque, absolute coefficient $C_Q = \frac{Q}{\rho n^2 D^5}$

P, Power, absolute coefficient $C_P = \frac{P}{\rho n^3 D^5}$

C_s, Speed-power coefficient $= \sqrt[5]{\frac{\rho V^5}{P n^2}}$

η, Efficiency

n, Revolutions per second, r.p.s.

Φ, Effective helix angle $= \tan^{-1}\left(\frac{V}{2\pi r n}\right)$

5. NUMERICAL RELATIONS

1 hp.=76.04 kg-m/s=550 ft-lb./sec.

1 metric horsepower=1.0132 hp.

1 m.p.h.=0.4470 m.p.s.

1 m.p.s.=2.2369 m.p.h.

1 lb.=0.4536 kg.

1 kg=2.2046 lb.

1 mi.=1,609.35 m=5,280 ft.

1 m=3.2808 ft.